

RESEARCH

Open Access



# Histone H3 lysine 9 tri-methylation is associated with pterygium

Dahee Choi<sup>1†</sup>, Ann-Yae Na<sup>1†</sup>, Seok-Won Jeoung<sup>1</sup>, Yun-Hee Choi<sup>2,3</sup>, Nayoon Park<sup>2</sup>, Hyun-Sun Park<sup>4</sup>, Hyuk-Kwon Kwon<sup>5</sup>, Hyun-Shik Lee<sup>1</sup>, Dong-Hyung Cho<sup>1</sup>, Dong Hyun Kim<sup>2\*</sup> and Hong-Yeoul Ryu<sup>1\*</sup>

## Abstract

**Background** Pterygium, abnormal growths of conjunctival tissue onto the cornea, are common ocular surface conditions with a high risk of recurrence after surgery and potential ophthalmic complications. The exact cause of pterygium remains unclear, and the triggers are still unknown. This study aims to investigate the relationship between pterygium and epigenetics to uncover the cause of pterygium and identify biomarkers for its diagnosis.

**Methods** We performed a ChIP-seq assay to compare genome-wide histone modification levels between normal conjunctiva and stage 3 pterygium samples.

**Results** In this study, we investigate the epigenetic profiles of patients with pterygium, focusing on histone H3 lysine 4 (H3K4) and lysine 9 (H3K9) trimethylation (me3). While H3K4me3 levels showed no significant genome-wide change, they were significantly altered in genes related to development and ocular diseases. Conversely, H3K9me3 levels were markedly elevated genome-wide, particularly at the promoters of 82 genes involved in developmental pathways. Furthermore, we identify six genes, *ANK2*, *AOAH*, *CBLN2*, *CDH8*, *CNTNAP4*, and *DPP6*, with decreased gene expression correlated with substantially increased H3K9me3, suggesting their potential as biomarkers for pterygium.

**Conclusion** This study represents the first report linking histone modification to pterygium progression, providing valuable insights into therapeutic strategies and potential drug targets.

**Keywords** Pterygium, Histone modification, H3K4me3, H3K9me3, Development, Biomarker

<sup>†</sup>Dahee Choi and Ann-Yae Na contributed equally to this work.

\*Correspondence:

Dong Hyun Kim  
amidfree@gmail.com  
Hong-Yeoul Ryu  
rhr4757@knu.ac.kr

<sup>1</sup>KNU G-LAMP Project Group, KNU Institute of Basic Sciences, School of Life Sciences, BK21 FOUR KNU Creative BioResearch Group, College of Natural Sciences, Kyungpook National University, Daegu 41566, South Korea

<sup>2</sup>Department of Ophthalmology, Korea University College of Medicine, 73, Goryeodae-ro, Seongbuk-gu, Seoul 02841, Republic of Korea

<sup>3</sup>School of Health and Environmental Science, Korea University, Seoul, South Korea

<sup>4</sup>Department of Pharmacology, Chonnam National University Medical School, Hwasun-gun, Jeonnam 58128, Republic of Korea

<sup>5</sup>Division of Life Science, Division of Bio & Medical Bigdata Department (BK4 Program), Gyeongsang National University, Jinju 52828, Republic of Korea



## Background

Pterygium, also known as surfer's eye, are common ocular surface formations characterized by the abnormal growth of conjunctiva tissue onto the cornea. The main factor of pterygium development is long-term exposure to UV radiation through sunlight, with other factors including viral infections, hereditary factors, and growth factors [1–6]. Without treatment, astigmatism, threatening the visual axis, and eye movement restriction may occur. Although surgical removal is the preferred treatment method, the recurrence rate varies from 2 to 88% [7]. The risk factors for recurrence include age, size of the pterygium tissues, and multiple recurrences [8, 9]. In view of the controversies on the multiple mechanisms of pterygium formation, studies have been carried out using high-throughput sequencing technologies to attempt to elucidate gene expression patterns that underlie molecular events of interest in its pathogenesis [10–12]. However, the pathogenesis of pterygium formation is yet to be fully understood, and the critical triggers therein are yet to be precisely described.

Histone modification is a well-known epigenetic mechanism involved in regulating gene expression [13]. Histones have N- and C-terminal tails which are often subjected to various post-translational modifications (PTMs), including acetylation, methylation, phosphorylation, ubiquitylation, and sumoylation [14, 15]. Histone methylation on lysine (K) residues can function to either activate or repress gene expression, depending on which lysine residues are methylated. In general, methylations at K4, K36, and K79 of histone H3 are involved in the activation of transcription, whereas methylations at K9 and K27 of histone H3 and at K20 of H4 are associated with gene repression [16].

Epigenetic influences on gene expression and genetic regulation play a critical role in development and cell differentiation [17, 18]. Some studies have shown a correlation between epigenetic modifications and various diseases, including cancer, autoimmune diseases, and ocular diseases [19–24]. For instance, histone modification, which remodels chromatin structure, thus regulating transcription, has been associated with diseases such

as Alzheimer's disease, atherosclerosis, and type 2 diabetes [25–28]. Additionally, recent studies found epigenetic modifications associated with different ocular diseases, for example, DNA methylation with cataracts, age-related macular degeneration, and Fuchs' endothelial corneal dystrophy [29–32]. In pterygium, several associated epigenetics modifications have been discovered, including the hypermethylation of the E-cadherin, *P15<sup>INK4b</sup>*, and *P16<sup>INK4a</sup>* gene promoters [33, 34]. Epigenetic treatments are emerging as a new approach to disease therapy [35, 36]. In one set of studies, researchers revealed the key role of epigenetic processes in regulating immune cell function and mediating anti-tumor immunity [37]. However, there is currently no evidence of an epigenetic correlation between histone methylation and pterygium formation.

Here, we explore the correlation between changes in H3K4 and H3K9 tri-methylation (me3) and gene expression in patients with pterygium to better understand pterygium pathogenesis. While the genome-wide H3K4me3 pattern shows no significant change in patients with pterygium, its levels were significantly altered in a number of genes associated with developmental processes or eye diseases. Conversely, H3K9me3 levels show genome-wide elevation in pterygium-affected patients. Specifically, H3K9me3 levels at the promoter regions of 82 genes involved in developmental pathways are significantly increased in pterygium sufferers. Comparing these findings with the gene expression profile associated with pterygium, we observe the downregulation of six of these genes, *ANK2*, *AOAH*, *CBLN2*, *CDH8*, *CNTNAP4*, and *DPP6*, which are closely linked to biomarkers for various human diseases. Therefore, we propose that these six identified H3K9me3-affected genes may represent potential biomarkers for future pterygium diagnosis.

## Methods

### Sample collection

Based on transparency, pterygium were classified into 3 morphological stages: stage 1 consists of atrophic pterygium, in which episcleral blood vessels are clearly visible; stage 2 consists of intermediate pterygium, which have characteristics between atrophic and fleshy pterygium; and stage 3 consists of fleshy pterygium, in which the episcleral vessels are completely obscured [38]. Four patients with a stage 3 pterygium participated in this study, and we collected conjunctival samples from 4 patients to represent healthy individuals. Normal conjunctival tissue was harvested from a conjunctival autograft obtained from the superotemporal quadrant of the bulbar conjunctiva of a patient with pterygium. These samples were obtained from Korea University Anam Hospital (Table 1) and approved by the Institutional Review Board (IRB) of the Korean University Anam Hospital (IRB number:

**Table 1** Genders and age groups of the eight participants

| No. | Pterygium stage | Gender | Age Group |
|-----|-----------------|--------|-----------|
| 1   | 3rd             | M      | 60–70     |
| 2   | 3rd             | F      | 60–70     |
| 3   | 3rd             | M      | 70–80     |
| 4   | 3rd             | F      | 70–80     |
| 5   | N/A             | M      | 60–70     |
| 6   | N/A             | F      | 60–70     |
| 7   | N/A             | M      | 70–80     |
| 8   | N/A             | F      | 70–80     |

N/A: conjunctiva sample, 3rd: stage 3 pterygium, M: Male, F: Female

No. 2022AN0503). We performed a retrospective analysis of patients who had been diagnosed with pterygium between November 3, 2022, and September 30, 2023.

### Chromatin Immunoprecipitation (ChIP)

ChIP experiments were performed as described previously with slight modifications [39–41]. Briefly, approximately 15 mg of tissue excised from participants was used for each ChIP sample. All samples were weighed and fixed in 1 ml of 1% formaldehyde in PBS on ice with slight shaking for 15 min. Before fixing, each tissue sample was chopped into 1 × 1 mm-sized chunks with razor blades. For quenching, 2 M glycine was added to cross-linked samples to a final concentration of 0.125 M. Cells were then lysed in cell lysis buffer (5 mM PIPES [pH 8.0], 1% Triton X-100, and 85 mM KCl) with inhibitors (0.5 mM DTT, 5 mM sodium butyrate, protease inhibitor cocktail [Roche, 4693132001], 1 mM PMSF [Roche, 11359061001], and PhosSTOP [Roche, PHOSS-RO]) and nuclei lysis buffer (50 mM Tris-HCl [pH 8.0], 10 mM EDTA [pH 8.0], and 1% SDS) with inhibitors. Chromatin sheared via sonication was diluted 4-fold with IP dilution buffer (50 mM Tris-HCl [pH 7.4], 1 mM EDTA [pH 8.0], 150 mM NaCl, 0.25% Na-deoxycholate, 1% Triton X-100) and incubated with protein A agarose beads (Cytiva, CL-4B) conjugated with anti-H3K4me3 (Abcam, 8580) or anti-H3K9me3 (Abcam, 8898) at 4 °C for 14 h for precipitation. The precipitates were then washed sequentially with wash buffer I (50 mM HEPES [pH 7.6], 0.1% SDS, 1% Triton X-100, 150 mM NaCl, and 0.1% Na-deoxycholate), wash buffer II (50 mM HEPES [pH 7.6], 0.1% SDS, 1% Triton X-100, 300 mM NaCl, and 0.1% Na-deoxycholate), wash buffer III (10 mM Tris-HCl [pH 8.0], 200 mM LiCl, 1 mM EDTA [pH 8.0], 0.5% NP-40, and 0.4% Na-deoxycholate), and wash buffer IV (10 mM Tris-HCl [pH 8.0] and 1 mM EDTA) and eluted at 65 °C with 50 mM Tris-HCl [pH 8.0], 10 mM EDTA, and 1% SDS) in TES buffer. Then, after the eluted chromatin fragments were treated with protease (Sigma-Aldrich, P5147), the DNA was extracted with QIAquick PCR purification kits (Qiagen, 28104) following the manufacturer's protocols.

### Data analysis

Sequencing libraries were constructed utilizing TruSeq DNA Sample prep kits according to the manufacturer's protocols (TruSeq ChIP Sample precipitation guide 15023092 Rev. B) and sequenced on an Illumina NovaSeq 6000 following the manufacturer's protocols [42]. Reads were trimmed using Trimmomatic (version 0.38) and aligned to the *Homo sapiens* reference genome (GRCh38) using BowTie (version 1.1.2). Peaks were called utilizing MACS2 (version 2.1.1.20160309), and duplicate reads were processed using Picard (version 0.118). The called peaks were then annotated in ChIPSeeker (version

1.16.1) using gene models from the National Center for Biotechnology Information (NCBI, <https://www.ncbi.nlm.nih.gov>). A comparative analysis of data was performed using csaw (version 1.34.0). Normalized bedGraph files were generated using MACS2 (command “-B-SPMR”) and then converted to bigwig files using the bedGraphToBigWig program. The genome-wide profile was generated using the tools in the deepTools suite (version 3.1.3). All gene ontology (GO) and Kyoto Encyclopedia of Genes and Genomes (KEGG) pathway analyses were performed utilizing the Database for Annotation, Visualization and Integrated Discovery (DAVID database; <https://david.ncifcrf.gov>). All GO and KEGG data were then filtered based on the EASE score, a modified Fisher's Exact *P*-value utilized by the DAVID database, removing any associations with an EASE score less than 0.1, and GO plots were created with the *ggplot2* (version 3.4.4) R library. A gene-to-gene interaction analysis was performed by utilizing GeneMANIA (<https://genemania.org>) to construct and analyze interactions between the analyzed genes. ChIP-seq tracks were viewed in the Integrative Genomics Viewer (IGV, <https://igv.org/>).

### RNA-seq source and analysis

We obtained RNA-seq data from NCBI (SRA file accession number PRJNA669964; <https://www.ncbi.nlm.nih.gov/sra>), which included data from three normal conjunctival tissue and three pterygium tissue samples. We then aligned the RNA-seq reads to the *Homo sapiens* reference genome (GRCh38). Gene expression was normalized with the *DESeq2* package in R (version 4.2.3), and up- and down-regulated genes were identified, considering *P*-values less than 0.05 to be statistically significant [43].

## Results

### H3K4me3-enriched genes are altered in patients with pterygium

Because, though a number of epigenetic modifications are associated with pterygium, a correlation with histone modification has not been yet reported, we performed a ChIP-seq assay to compare genome-wide H3K4me3 levels between normal, healthy conjunctiva and stage 3 pterygium samples (Fig. 1 and Supplementary Fig. 1). Consistent with previous results [44, 45], H3K4me3 was preferentially distributed at promoter regions in both samples, with only a slight decrease in the proportion of H3K4me3-enriched promoters in pterygium (Fig. 1A). Also, the majority of the 11,256 H3K4me3 peaks observed in the normal conjunctiva were still present in pterygium (10,659 peaks, 95%) (Fig. 1B). Although a slight increase in H3K4me3 at the peak center and a slight decrease in both the gene body and transcription end site were observed in pterygium (Fig. 1C), a *K*-means cluster analysis targeting three clusters with distinct

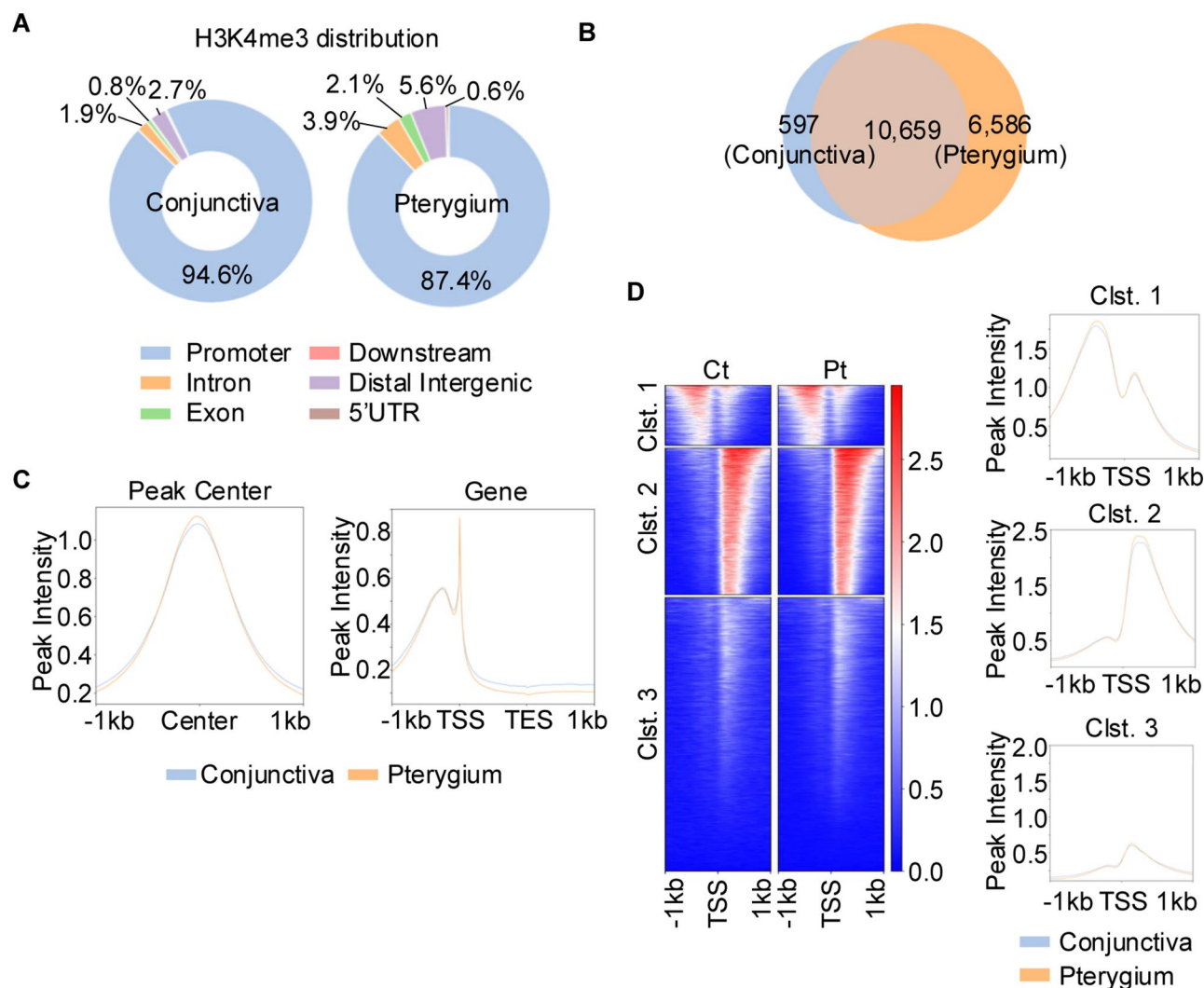


**Fig. 1** Analysis of genome-wide H3K4me3 levels in patients with pterygium. **(A)** Summaries of genome-wide ChIP-seq data of H3K4me3 in normal conjunctiva (left) and pterygium (right). The pie chart shows the distribution of H3K4me3 peaks at promoter, intron, exon, downstream, distal intergenic, and 5' untranslated (UTR) regions. Numbers indicate the percentages of detected sites. **(B)** A Venn diagram of the H3K4me3 peaks displayed in A. The areas of the subsets are proportional to the number of detected H3K4me3 peaks. **(C)** A ChIP read-density profile of the data shown in A. The profile plots show the average ChIP signals in  $\pm 1$  kb windows relative to the center of peaks (left) and from transcription start sites (TSSs) and transcription end sites (TESs) (right). **(D)** A clustered heatmap (left) and ChIP read-density profile (right) of the ChIP-seq data shown in A. The H3K4me3 peaks across TSSs with  $\pm 1$  kb are separated into three clusters by K-means clustering (Ct: conjunctiva, Pt: pterygium, C1st.: cluster)

H3K4me3 peak patterns did not reveal a significant change in the H3K4me3 distribution (Fig. 1D). Therefore, our data show that the genome-wide H3K4me3 pattern was not greatly altered in patients with stage 3 pterygium.

Next, we carried out a more detailed assessment of the difference in H3K4me3 signal intensity between the two groups (Fig. 2). A comparison of the ChIP-seq profiles from both groups revealed 434 significantly increased peaks and 490 significantly decreased peaks in pterygium (Fig. 2A). Significantly increased peaks associated with H3K4me3 were predominantly located at promoter regions (93.5%), while the significantly decreased peaks were more broadly distributed (promoter: 62.8%, intron: 18.9%, and intergenic: 16.1%) (Fig. 2B). Next, we

performed a GO analysis to determine the H3K4me3-governed genes and pathways involved in pterygium pathogenesis (Fig. 2C and D). The top 5 most highly enriched GO terms for H3K4me3 upregulated genes were “endocytosis,” “in utero embryonic development,” “adenosine to inosine editing,” “multicellular organism growth,” and “apoptotic process.” In H3K4me3 downregulated genes, the top 5 most enriched GO terms were “commitment of neuronal cell to specific neuron type in forebrain,” “heterophilic cell–cell adhesion via cell adhesion molecules (CAMs),” “neuron migration,” “regulation of cell proliferation,” and “dentate gyrus development.” Notably, the top 5 enriched GO terms associated with genes with H3K4me3-altered expression include

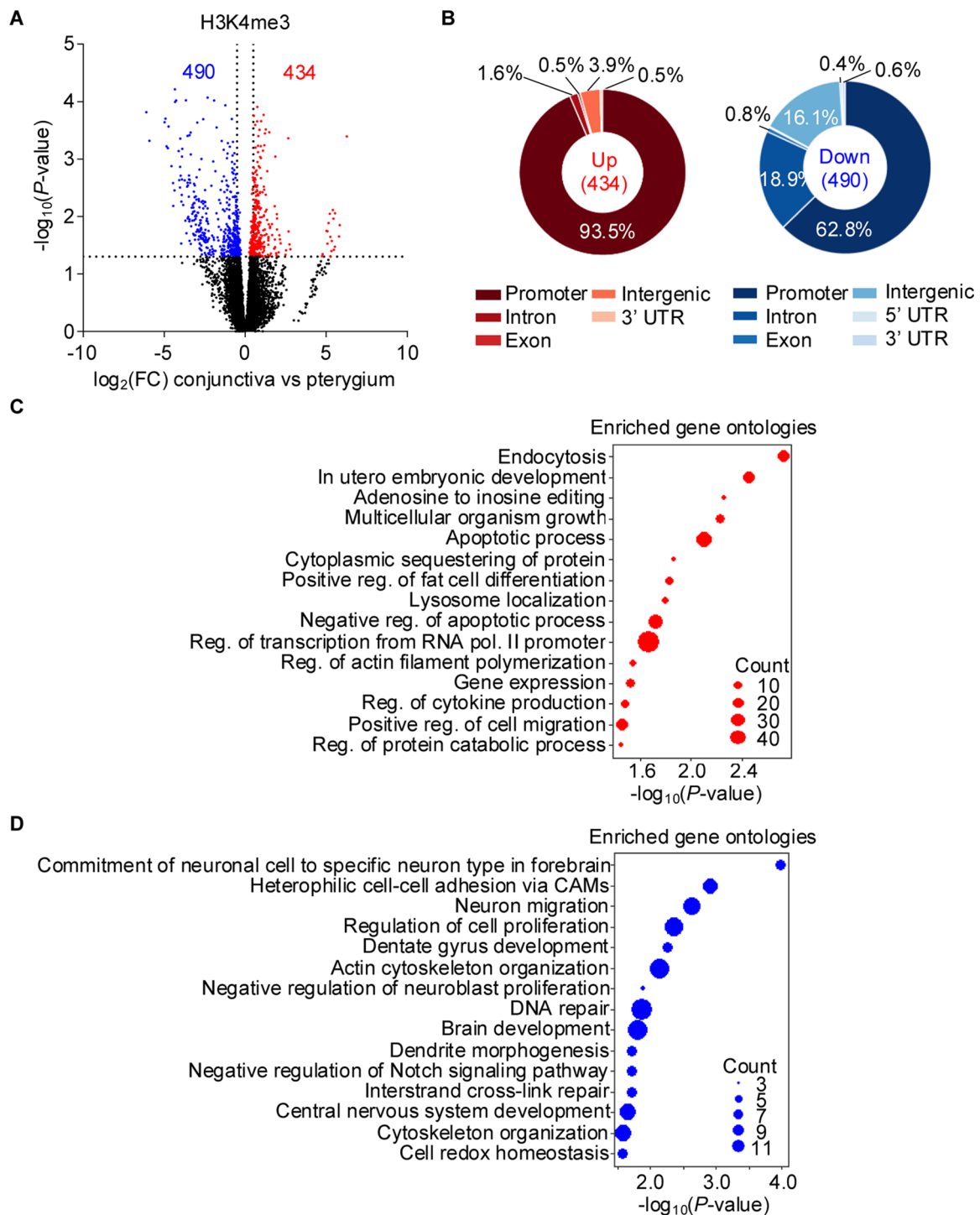


**Fig. 2** Gene ontology (GO) analysis of significantly upregulated and downregulated H3K4me3 signals in patients with pterygium. **(A)** A volcano plot representing the differential binding analysis of the H3K4me3 ChIP-Seq data from pterygium and healthy conjunctiva. The y-axis represents the mean of the negative logarithm of the *P*-values, and the x-axis corresponds the  $\log_2$ (fold change [FC]) values. Red and blue dots denote sites significantly changed (*P*-value < 0.05) by  $\log_2(\text{FCs}) > 1.5$  or  $< -1.5$  (i.e., with differentially greater or lower trimethylation), respectively, and black dots denote sites with statistically insignificant changes. The red and blue numbers indicate the number of red and blue dots, respectively. **(B)** Pie charts describing the distribution of peaks with significantly increased (left) and decreased (right) H3K4me3 signals, corresponding to the red and blue dots in A, respectively, as shown in Fig. 1A. The numbers in parentheses indicate the total number of genes used in the analysis. **(C and D)** Enriched GO analysis terms for the genes with significantly increased **(C)** and decreased **(D)** H3K4me3 shown in A. The circle size represents the number of genes in the significant gene list associated with the GO term. The x-axis corresponds to the  $-\log_{10}(P\text{-values})$

pathways related to development or eye diseases, such as apoptosis [46].

### H3K9me3 levels are significantly increased in patients with pterygium

The H3K4me3 is typically associated with gene activation and euchromatin regions, while H3K9me3 is linked to gene repression and heterochromatin regions [47–49]. The dynamic interplay between these two modifications considerably influences chromatin state and gene expression regulation [50]. Therefore, we next

investigated the genome-wide effects of H3K9me3 in patients with stage 3 pterygium (Fig. 3 and Supplementary Fig. 1). Corroborating the results of previous studies [26, 51], H3K9me3 was predominantly observed at gene body and intergenic regions in both normal conjunctiva and pterygium samples (Fig. 3A). In addition, out of the 22,450 total H3K9me3 peaks in normal conjunctiva, 85% (19,077 peaks) remained present in pterygium (Fig. 3B). Although the distribution of H3K9me3 ChIP-seq enrichment at the peak center did not show a significant change in pterygium (Fig. 3C left panel and D), a notable increase

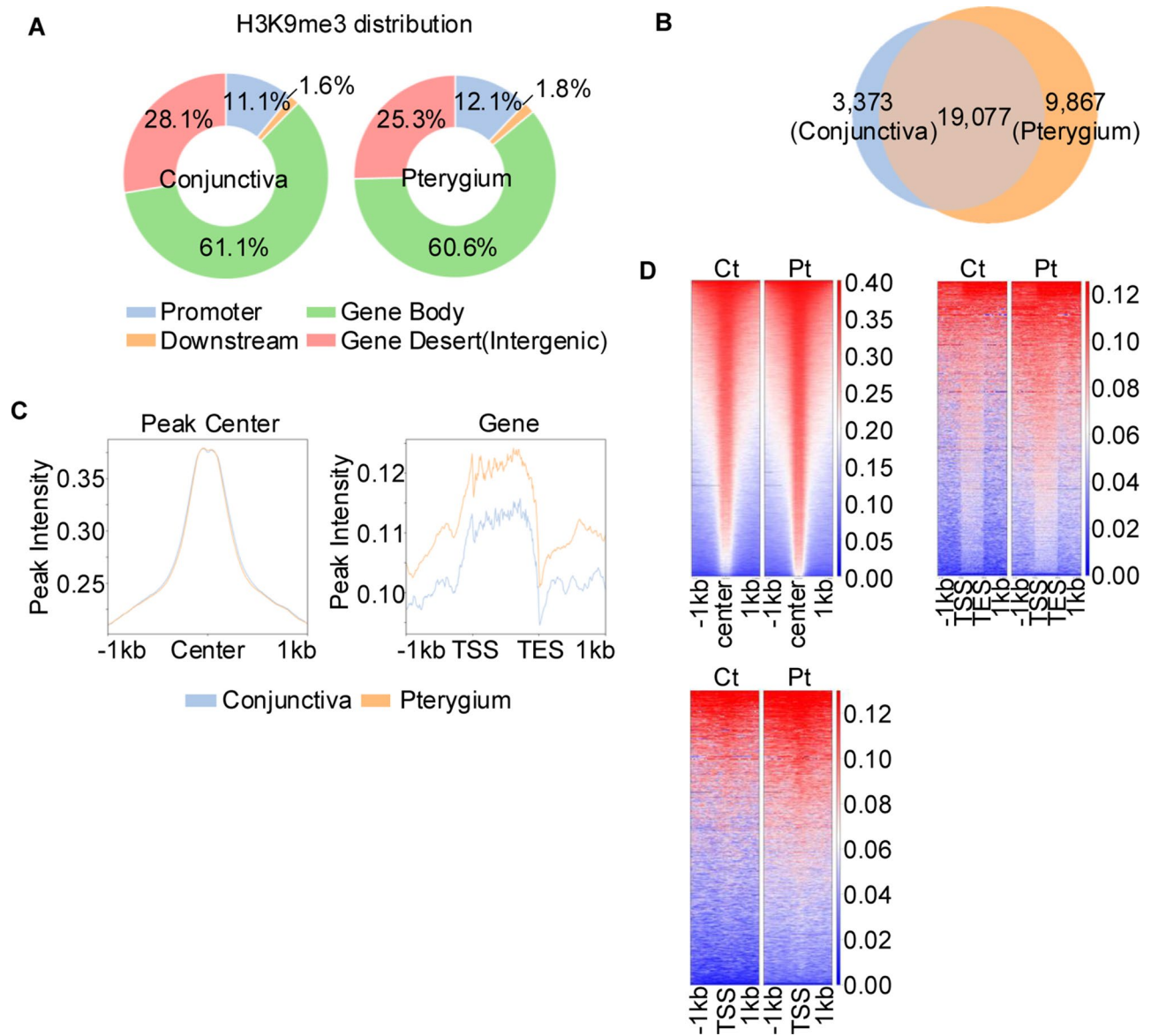


**Fig. 3** Patients with pterygium exhibit increased H3K9me3 levels across genes. **(A)** Summaries of genome-wide ChIP-seq data of H3K9me3 in normal conjunctiva (left) and pterygium (right), with details following those of Fig. 1A. The pie chart shows the distribution of H3K9me3 peaks in promoter, downstream, gene body, and gene desert (intergenic) regions. **(B)** A Venn diagram of the H3K9me3 peaks displayed in A, with details following those of Fig. 1B. **(C)** A ChIP read-density profile of the data shown in A, with details following those of Fig. 1C. **(D)** A heatmap of the H3K9me3 ChIP-seq peaks of the data shown in A across  $\pm 1$  kb windows relative to the center of peaks (upper left), from TSS to TES (upper right), and across  $\pm 1$  kb windows relative to the TSS (bottom)

of H3K9me3 from transcription start site (TSS) to transcription end site was observed (Fig. 3C right panel and D), suggesting that H3K9me3 is a critical epigenetic factor for the regulation of gene expression in patients with pterygium.

Subsequently, we carried out a comprehensive analysis of the H3K9me3 ChIP-seq profiles of both tissue groups to examine the differential H3K9me3 peaks (Fig. 4), identifying 1,822 peaks with significantly increased intensity and 2,539 peaks with significantly decreased intensity in pterygium (Fig. 4A). The GO analysis revealed that H3K9me3-governed genes are involved in a variety of pathways, such as “regulation of transcription,” “modulation of synaptic transmission,” “signal transduction,” “neuron cell–cell adhesion,” and “nervous system development” (Supplementary Fig. q), implying that H3K9me3 may play an important role in the transcription regulation of genes affecting these diverse pathways. Most of the sites showing significantly changed peaks associated with H3K9me3 were within the gene body and intergenic regions (more than 90%), with a small proportion of signals at the promoter region (about 6–7%) (Fig. 4B). However, a substantial increase, over 10-fold, in H3K9me3 was found at the promoter regions of 82 genes with high fold change (FC) values in pterygium (Fig. 4C), suggesting that abnormally enhanced H3K9me3 at the promoter regions lead to dysfunctional transcription initiation in pterygium.

Next, we analyzed the genetic interaction network of these 82 high FC genes using GeneMANIA (Fig. 4D). The results showed that 47 of the genes are correlated based on their co-expression and pathway interactions. Notably, we found that developmental pathways, including ectoderm differentiation and development, are key targets of H3K9me3-driven regulation in pterygium. Taken together, our data indicate that H3K9me3 is clearly increased at the promoter regions of genes related to developmental processes in patients with pterygium.

#### **Integrative analysis of H3K9me3 ChIP-seq and RNA-seq data identified six target genes in patients with pterygium**

Various genome-wide RNA analyses have shown that H3K9me3 is associated with gene repression [52–54]. Therefore, we directly compared the ChIP-seq data of H3K9me3 with RNA-seq data sets obtained from Liu et al. [55], observing significant changes in pterygium (Fig. 5). Specifically, 9.7% of genes (359 out of a total of 3,684 genes) with significantly altered H3K9me3 peaks (4,361 peaks in Fig. 4A) in pterygium overlapped with differentially expressed genes in the RNA-seq data (6,062 genes) in pterygium (Fig. 5A). Among the 359 overlapping genes, 138 and 221 genes were up- and down-regulated by H3K9me3, respectively (Fig. 5B). In a scatter plot of the ChIP-seq and RNA-seq data, 41 genes in the

first quadrant and 97 genes in the second quadrant indicate H3K9me3-enhanced up- and down-regulated genes, respectively. Conversely, 147 and 74 genes were H3K9me3-diminished differentially down- and up-regulated genes, respectively.

Because H3K9me3 usually contributes to the silencing of genes [43], we focused on analyzing the 97 down-regulated genes that showed a significant increase in H3K9me3. The top 5 enriched GO terms for these 97 genes were “cell adhesion,” “phagocytosis,” “modulation of synaptic transmission,” “regulation of presynapse assembly,” and “cell–cell adhesion” (Fig. 5C, sky blue circles). Also, pathways such as “cell adhesion molecules,” “transcriptional misregulation in cancer,” and “malaria” are represented in KEGG pathway analysis (Fig. 5C, orange circles). A binding motif analysis of the 97 genes identified, among others, ZN770, SP4, ZN768, ZN264, FOXJ3, PRDM6, and LEF1, all of which involve zinc finger domains or function as transcription factors (Fig. 5D). Notably, among the 97 genes, six, *ANK2*, *AOAH*, *CBLN2*, *CDH8*, *CNTNAP4*, and *DPP6*, are included in the group of high FC genes identified in Fig. 4A (Fig. 5B). These six genes are closely related to human diseases, such as breast cancer, acute ethmoiditis and chronic frontal sinusitis, HPV infection, Parkinson’s disease, and pancreatic ductal adenocarcinoma (Table 2), suggesting that H3K9me3-mediated regulation of these genes is critical for pathogenesis. In conclusion, our data suggest that increased H3K9me3-mediated repression of these six target genes may be causative factors in pterygium development.

#### **Discussion**

Epigenetics is important in the regulation of gene expression and can be used as biomarkers in diverse human diseases [56]. However, to our knowledge, there are no studies on histone modification in patients with pterygium. Therefore, in this study, we provide initial evidence that H3K4 and H3K9 methylation are closely related to the pathogenesis of pterygium.

The genome-wide ChIP-seq analysis for H3K4me3 showed both increases and decreases in H3K4me3 levels at promoter regions in patients with pterygium (Fig. 2A and B). Notably, three GO terms for H3K4me3-upregulated genes, endocytosis, adenosine to inosine editing, and apoptotic process, have been significantly related to eye diseases (Fig. 2C) [46, 57, 58]. Our data thus suggest that these three pathways may affect the occurrence of pterygium. However, the pathogenesis of pterygium remains unclear, and another study reported decreased levels of H3K4me3 in aging photoreceptors [59]. Therefore, further studies are needed to elucidate the exact correlation between H3K4me3 and pterygium formation

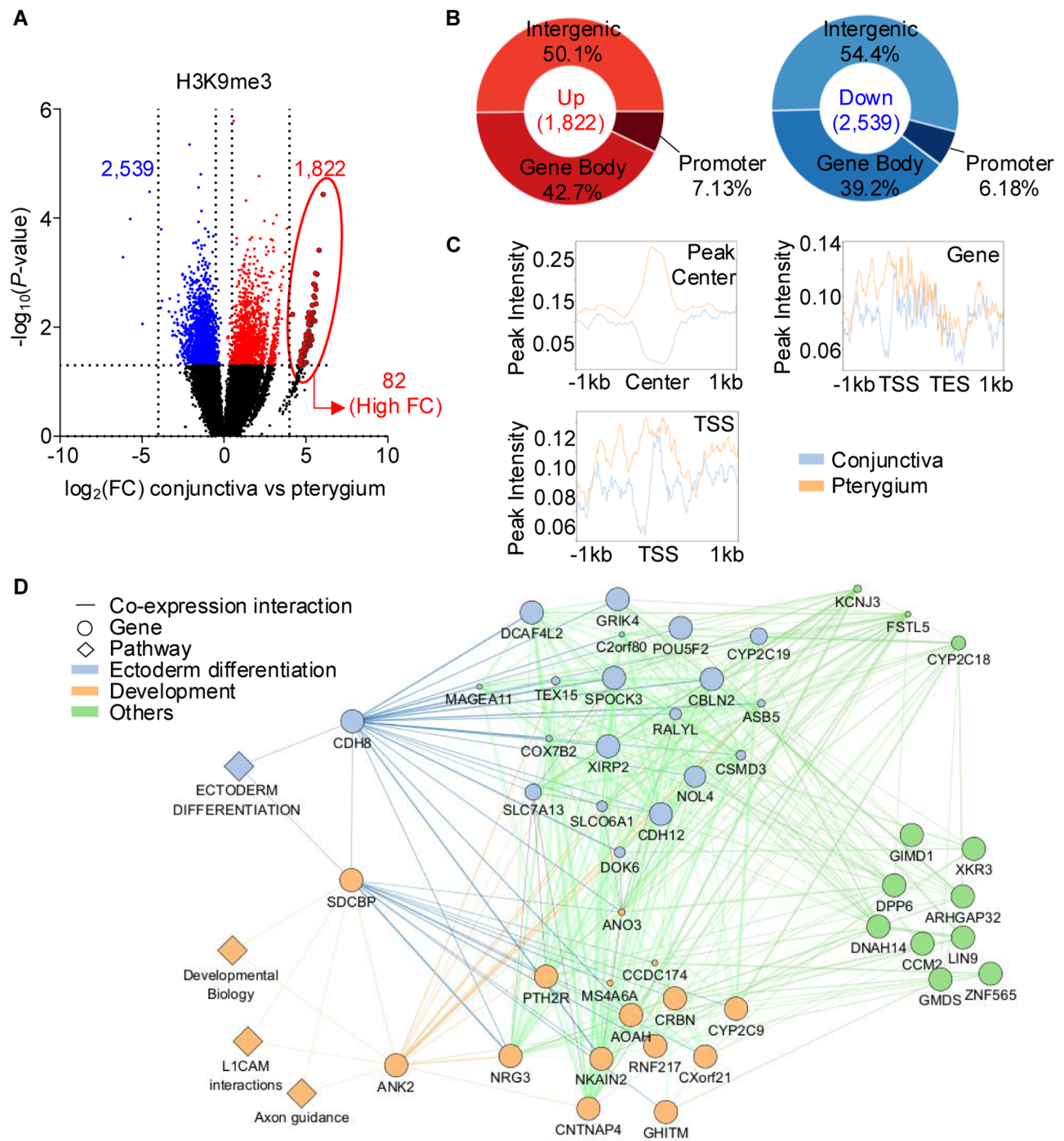


**Fig. 4** H3K9me3 levels are increased in genes involved in ectoderm differentiation and developmental pathways. **(A)** A volcano plot displaying H3K9me3 alterations in pterygium and healthy conjunctiva, with details following those of Fig. 2A. Circles indicate the 82 genes with high FC values. **(B)** Pie charts showing the distribution of peaks with significantly increased (left) and decreased (right) H3K9me3 signals, corresponding to the red and blue dots in A, with details following those of Fig. 2B. **(C)** A ChIP read-density profile of H3K9me3 in genes with high FC values, corresponding to those identified in A across  $\pm 1$  kb windows relative to the center of peaks (upper left), from TSS to TES (upper right), and across  $\pm 1$  kb windows relative to the TSS (bottom left). **(D)** A co-expression network of genes with high FC values (analyzed using GeneMANIA; <http://genemania.org>), corresponding to those identified in A. Lines, circles, and diamonds indicate co-expression interactions, genes, and pathways, respectively. The circle size represents the strength of the interaction. Sky blue, orange, and green colors represent pathways related to ectoderm differentiation, development, and others, respectively

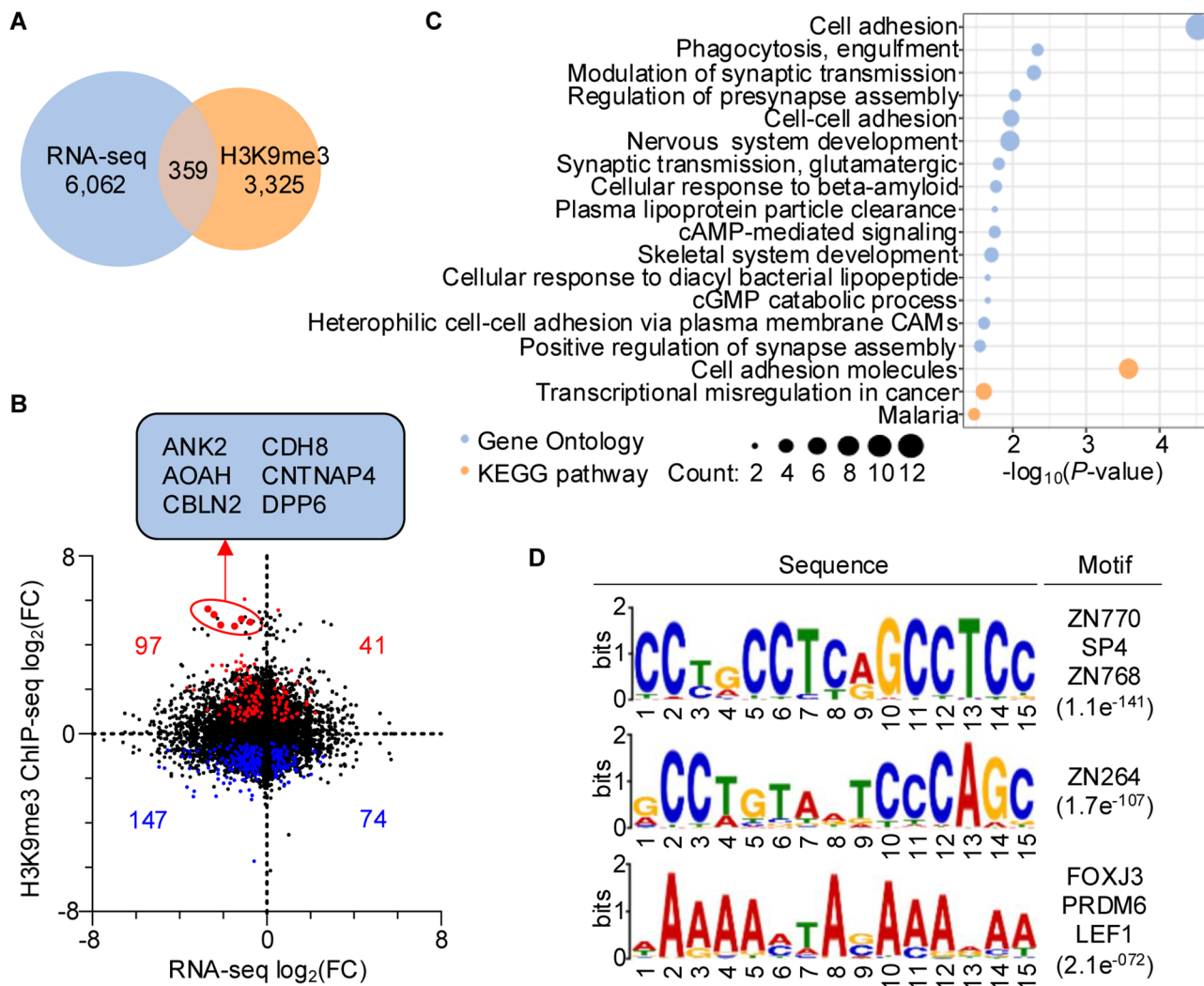


**Fig. 5** Comparison of the H3K9me3 ChIP-seq profiles with publicly available RNA-seq data from patients with pterygium. **(A)** A Venn diagram showing the overlap between genes with significant, > 1.5-fold H3K9me3 signal changes and with differential expression in patients with pterygium. Details follow those of Fig. 1B. **(B)** A scatter plot of ChIP-seq (y-axis) and RNA-seq (x-axis) signals in the overlapping genes in A. Significantly up-regulated H3K9me3-affected genes are shown in red and significantly down-regulated H3K9me3-affected genes are shown in blue ( $P$ -value < 0.05). Genes with high FC values ( $FC > 10$ ) are circled and gene symbols are listed inside the box. **(C)** Enriched GO terms (sky blue) and KEGG pathways (orange) associated with genes showing both significantly increased H3K9me3 and decreased expression in pterygium. The circle size represents the number of genes associated with the GO term or KEGG pathway. The x-axis corresponds to the  $-\log_{10}(P\text{-values})$ . **(D)** The sequence motifs enriched in the genes identified in C. The frequency of motif occurrence, alignment quality ( $e$ -value), and transcription factors potentially recognizing the motif are displayed for each motif

**Table 2** Summary of biomarker-related target diseases for the six identified genes in this study

| Gene    | Target disease                                       | Reference |
|---------|--|-----------|
| ANK2    | Breast cancer  | [71]      |
| AOAH    | Acute lung injury, asthma and chronic rhinosinusitis | [73–75]   |
| CBLN2   | Colon adenocarcinoma                                 | [72]      |
| CDH8    | HPV infection  | [69]      |
| CNTNAP4 | Parkinson's disease                                  | [76, 77]  |
| DPP6    | Pancreatic ductal adenocarcinoma                     | [78]      |

as well as the underlying mechanism of pterygium pathogenesis.

Interestingly, we identified 82 genes, primarily involved in developmental pathways, with a remarkable increase in H3K9me3 in pterygium (Fig. 4A and D). In general, developmental pathways are divided into various sub-pathways, each performing different roles within the cell. For example, Notch signaling plays a critical role in corneal wound healing [60]. Mutations in the adenomatous polyposis coli protein led to the overactivation of the Wnt/ $\beta$ -catenin signaling pathway, resulting in the development of colorectal cancer [61]. Additionally, AMPK signaling regulates the tumor suppressor protein

**Table 3** Comparison of the six identified genes between our study and reference data

| Gene | Reference | Regulatoin | Number of Samples           |
|------|-----------|------------|-----------------------------|
| ANK2 | [63]      | Down       | Conjunctiva 8, Pterygium 8  |
| ANK2 | [64]      | Down       | Conjunctiva 4, Pterygium 4  |
| AOAH | [65]      | Down       | Conjunctiva 10, Pterygium 8 |

p53 and, thus, regulates tumor suppression [62]. Errors in developmental pathways can lead to severe diseases or cellular dysfunctions. Therefore, defects in developmental pathways caused by excessive increases of H3K9me3 in pterygium could be critical to their pathogenesis.

We identified the six target genes that were particularly affected by increased H3K9me3-mediated suppression, *ANK2*, *AOAH*, *CBLN2*, *CDH8*, *CNTNAP4*, and *DPP6* (Fig. 5B). Notably, comparisons with other RNA-seq datasets consistently revealed an identical pattern, with the downregulation of *ANK2* and *AOAH* closely aligning with our findings and supporting the validity of our observations. These consistent results indicate the reproducibility of the observed downregulation across independent datasets (Table 3) [63–65]. Among these, Ankyrin-B (AnkB) is a well-known key adaptor protein that connects cytoskeletal components such as  $\beta$ -spectrin and actin to membrane proteins, including ion channels, receptors, and cell adhesion molecules, in lens fiber cells. AnkB facilitates the membrane anchoring of Periaxin (Prx) and plays a crucial role in maintaining the morphology, alignment, membrane organization, and biomechanical properties of lens fiber cells [66]. Considering these functions, increased expression of AnkB could potentially affect the cytoskeletal structure and function of lens fiber cells, contributing to pathological changes observed in diseases such as pterygium. *CNTNAP4* and *DPP6* genes are related to eye disorders [67, 68]. *CNTNAP4* is a critical gene associated with the pathogenesis of primary open-angle glaucoma [69] and corneal diseases. It is strongly linked to increased corneal thickness (CCT), protective effects against POAG, and neural cell interactions, highlighting its importance in ocular health and disease mechanisms [67]. Additionally, *CNTNAP4* has been directly associated with natural variations in corneal thickness and is likely to play a pivotal role in regulating corneal structure alongside other genes such as *NTM*, *COL5A1*, and *COL8A2* [70]. These findings suggest that *CNTNAP4* holds potential as a biomarker for ocular disorders, particularly in conditions involving corneal integrity and glaucoma. The expression of *DPP4* is elevated in retinal pigment epithelium (RPE) cells and the Bruch's membrane, regions where degenerative deposits of waste materials and proteins accumulate to form drusen [68]. While the primary mechanisms are not yet fully understood, *DPP4* is proposed to potentially contribute to the formation of pterygium. Although these

genes are primarily associated with ocular disorders, their roles in systemic diseases underscore their broader biomarker potential. For instance, recent studies suggested that *ANK2* and *CBLN2* serve as biomarkers in breast cancer and colon adenocarcinoma, respectively [71, 72]. Diseases associated with *AOAH* include acute lung injury, asthma and chronic rhinosinusitis [73–75]. Additionally, the DNA methylation patterns of *CDH8* are possible biomarkers for detecting pathological changes associated with human papillomavirus (HPV) infection [69]. The proteins *CNTNAP4* and *DPP6* are also considered biomarkers; *CNTNAP4* deficiency may initiate phenotypes of Parkinson's disease, and hypermethylation of the *DPP6* promoter has been observed in patients with pancreatic ductal adenocarcinoma [76–78]. Furthermore, Several research groups have been trying to identify possible biomarkers for pterygium formation, with the most notable results pointing to heparin-binding epidermal growth factor (HB-EGF) [79]. Therefore, these six identified target genes will likely serve as new potential biomarkers for pterygium formation and could be further considered as new drug targets for treatments.

Our study concentrated on the analysis of two histone methylation modifications: H3K4me3 and H3K9me3. Nevertheless, other epigenetic modifications, including histone acetylation, sumoylation, and ubiquitination, are also crucial in the regulation of gene expression. Future research presents an opportunity to investigate additional epigenetic regulators involved in pterygium.

## Conclusions

To our knowledge, this is the first trial to investigate the correlation between histone modifications H3K4me3 and H3K9me3 and pterygium. Notably, H3K9me3 levels were significantly increased in patients with pterygium, and we identified six H3K9me3-governed target genes as potential biomarkers. This study provides a foundation for future research on the prevention and recurrence of pterygium.

## Abbreviations

|        |   |
|--------|---|
| CAMs   | Cell adhesion molecules   |
| ChIP   | Chromatin immunoprecipitation                                   |
| Clst   | Cluster   |
| Ct     | Conjunctiva   |
| DAVID  | Database for Annotation, Visualization and Integrated Discovery |
| FC     | Fold change   |
| GEO    | Gene Expression Omnibus   |
| GO     | Gene Ontology   |
| HB-EGF | Heparin-binding epidermal growth factor                         |
| HPV    | Human papillomavirus  |
| IRB    | Institutional Review Board                                      |
| KEGG   | Kyoto Encyclopedia of Genes and Genomes                         |
| KEITI  | Korean Environmental Industry & Technology Institute            |
| MOE    | Korean Ministry of Environment                                  |
| MSIT   | South Korea government  |
| NRF    | National Research Foundation of Korea                           |
| Pt     | Pterygium   |
| PTM    | Post-translational modification                                 |

TES Transcription end site  
TSS Transcription start site  
UTR Untranslated

## Supplementary Information

The online version contains supplementary material available at <https://doi.org/10.1186/s12886-025-03939-7>.

Supplementary Material 1

## Acknowledgements

None.

## Author contributions

D. C. contributed to the writing of the original draft, investigation, and formal analysis. A.Y.N. was involved in writing the original draft and conducting formal analysis. S.W.J. participated in investigation and formal analysis, while Y.H.C. and N.P. focused on investigation. H.S.P. and H.K.K. were responsible for formal analysis. H.S.L. and D.H.C. worked on writing, specifically in the review and editing stages. D.H.K. provided resources and acquired funding. Finally, H.Y.R. contributed to writing through review and editing, supervised the project, acquired funding, curated data, and was involved in conceptualization.

## Funding

This study was supported by a National Research Foundation of Korea (NRF) grant funded by the South Korea government (MSIT) [RS-2023-00212894], the Korea Basic Science Institute (National Research Facilities and Equipment Center) grant funded by the Korea government (MSIT) [RS-2024-00404285], a Learning & Academic Research Institution for Master's/PhD Students, and Postdocs Program of the National Research Foundation of Korea (NRF) grant funded by the Ministry of Education [RS-2023-00301914], and the Korean Environmental Industry & Technology Institute (KEITI) through the Core Technology Development Project for Environmental Diseases Prevention and Management funded by Korean Ministry of Environment (MOE) [no. 2022003310001].

## Data availability

Data generated in this publication have been deposited in Gene Expression Omnibus (GEO) with accession numbers: GSE272511 (token: ongzgyeufjavpwn).

## Declarations

### Ethics approval and consent to participate

Informed consents were obtained from all participants. The study adhered to the principles outlined in the Declaration of Helsinki and received approval from the Institutional Review Boards of Korea University Anam Hospital (IRB No. 2022AN0503).

### Consent for publication

Not applicable.

### Competing interests

The authors declare no competing interests.

Received: 3 September 2024 / Accepted: 19 February 2025

Published online: 03 March 2025

## References

- Moran DJ, Hollows FC. Pterygium and ultraviolet radiation: a positive correlation. *Br J Ophthalmol*. 1984;68:343–6. <https://doi.org/10.1136/bjo.68.5.343>.
- Al-Bdour M, Al-Latayfeh MM. Risk factors for pterygium in an adult Jordanian population. *Acta Ophthalmol Scand*. 2004;82:64–7. <https://doi.org/10.1046/j.1600-0420.2003.0213.x>.
- Anguria P, Kitinya J, Ntuli S, Carmichael T. The role of heredity in pterygium development. *Int J Ophthalmol*. 2014;7:563–73. <https://doi.org/10.3980/j.issn.2222-3959.2014.03.31>.
- Jacklin HN. FAMILIAL PREDISPOSITION TO PTERYGIUM FORMATION; REPORT OF A FAMILY. *Am J Ophthalmol*. 1964;57:481–2. [https://doi.org/10.1016/0002-9394\(64\)92668-6](https://doi.org/10.1016/0002-9394(64)92668-6).
- Chalkia AK, Spandidos DA, Deterakis ET. Viral involvement in the pathogenesis and clinical features of ophthalmic pterygium (Review). *Int J Mol Med*. 2013;32:539–43. <https://doi.org/10.3892/ijmm.2013.1438>.
- Gumus K, Karakucuk S, Mirza GE, Akgun H, Arda H, Oner AO. Overexpression of vascular endothelial growth factor receptor 2 in pterygia May have a predictive value for a higher postoperative recurrence rate. *Br J Ophthalmol*. 2014;98:796–800. <https://doi.org/10.1136/bjophthalmol-2012-301944>.
- Hirst LW. The treatment of pterygium. *Surv Ophthalmol*. 2003;48:145–80. [https://doi.org/10.1016/s0039-6257\(02\)00463-0](https://doi.org/10.1016/s0039-6257(02)00463-0).
- Lewallen S. A randomized trial of conjunctival autografting for pterygium in the tropics. *Ophthalmology*. 1989;96:1612–4. [https://doi.org/10.1016/s0161-6420\(89\)32667-4](https://doi.org/10.1016/s0161-6420(89)32667-4).
- Mahar P, Manzar N. Risk factors involved in pterygium recurrence after surgical excision. *Pakistan J Ophthalmol*. 2014;30. <https://doi.org/10.36351/pjo.v30.i2.285>.
- Ramasamy A, Mondry A, Holmes CC, Altman DG. Key issues in conducting a meta-analysis of gene expression microarray datasets. *PLoS Med*. 2008;5:e184. <https://doi.org/10.1371/journal.pmed.0050184>.
- Tseng GC, Ghosh D, Feingold E. Comprehensive literature review and statistical considerations for microarray meta-analysis. *Nucleic Acids Res*. 2012;40:3785–99. <https://doi.org/10.1093/nar/gkr1265>.
- Liu J, Ding X, Yuan L, Zhang X. Identification of pterygium-related mRNA expression profiling by microarray analysis. *Eye*. 2017;31:1733–9. <https://doi.org/10.1038/eye.2017.116>.
- Chou KY, Lee JY, Kim KB, Kim E, Lee HS, Ryu HY. Histone modification in *Saccharomyces cerevisiae*: A review of the current status. *Comput Struct Biotechnol J*. 2023;21:1843–50. <https://doi.org/10.1016/j.csbj.2023.02.037>.
- Ryu HY, Hochstrasser M. Histone sumoylation and chromatin dynamics. *Nucleic Acids Res*. 2021;49:6043–52. <https://doi.org/10.1093/nar/gkab280>.
- Choi J, Ryoo ZY, Cho DH, Lee HS, Ryu HY. Trans-tail regulation-mediated suppression of cryptic transcription. *Exp Mol Med*. 2021;53:1683–8. <https://doi.org/10.1038/s12276-021-00711-x>.
- Sims RJ 3rd, Nishioka K, Reinberg D. Histone lysine methylation: a signature for chromatin function. *Trends Genet*. 2003;19:629–39. <https://doi.org/10.1016/j.tig.2003.09.007>.
- Wu H, Sun YE. Epigenetic regulation of stem cell differentiation. *Pediatr Res*. 2006;59:r21–25. <https://doi.org/10.1203/01.pdr.0000203565.76028.2a.r>.
- Gibney ER, Nolan CM. Epigenetics and gene expression. *Heredity (Edinb)*. 2010;105:4–13. <https://doi.org/10.1038/hdy.2010.54>.
- Koch A, Joosten SC, Feng Z, de Ruijter TC, Draht MX, Melotte V, Smits KM, Veeck J, Herman JG, Van Neste L, et al. Analysis of DNA methylation in cancer: location revisited. *Nat Rev Clin Oncol*. 2018;15:459–66. <https://doi.org/10.1038/s41571-018-0004-4>.
- Ni Y, Zhang H, Chu L, Zhao Y. m6A Modification-Association with oxidative stress and implications on eye diseases. *Antioxid (Basel)*. 2023;12. <https://doi.org/10.3390/antiox12020510>.
- Zhong Q, Kowluru RA. Role of histone acetylation in the development of diabetic retinopathy and the metabolic memory phenomenon. *J Cell Biochem*. 2010;110:1306–13. <https://doi.org/10.1002/jcb.22644>.
- Hewagama A, Richardson B. The genetics and epigenetics of autoimmune diseases. *J Autoimmun*. 2009;33:3–11. <https://doi.org/10.1016/j.jaut.2009.03.007>.
- Li E, Choi J, Sim HR, Kim J, Jun JH, Kyung J, Ha N, Kim S, Ryu KH, Chung SS, et al. A novel HDAC6 inhibitor, CKD-504, is effective in treating preclinical models of Huntington's disease. *BMB Rep*. 2023;56:178–83. <https://doi.org/10.5483/BMBRep.2022-0157>.
- Kim U, Lee DS. Epigenetic regulations in mammalian cells: roles and profiling techniques. *Mol Cells*. 2023;46:86–98. <https://doi.org/10.14348/molcells.2023.0013>.
- Kadakol A, Malek V, Goru SK, Pandey A, Gaikwad AB. Telmisartan and Esculetin combination ameliorates type 2 diabetic cardiomyopathy by reversal of H3, H2A, and H2B histone modifications. *Indian J Pharmacol*. 2017;49:348–56. [https://doi.org/10.4103/ijp.JIP\\_710\\_16](https://doi.org/10.4103/ijp.JIP_710_16).
- Lee MY, Lee J, Hyeon SJ, Cho H, Hwang YJ, Shin JY, McKee AC, Kowall NW, Kim JI, Stein TD, et al. Epigenome signatures landscaped by histone H3K9me3 are

- associated with the synaptic dysfunction in Alzheimer's disease. *Aging Cell*. 2020;19:e13153. <https://doi.org/10.1111/acer.13153>.
27. Wang J, Xu X, Li P, Zhang B, Zhang J. HDAC3 protects against atherosclerosis through inhibition of inflammation via the microRNA-19b/PPAR $\gamma$ /NF- $\kappa$ B axis. *Atherosclerosis*. 2021;323:1–12. <https://doi.org/10.1016/j.atherosclerosis.2021.02.013>.
  28. Santana DA, Smith MAC, Chen ES. Histone Modifications in Alzheimer's Disease. *Genes (Basel)*. 2023;14. <https://doi.org/10.3390/genes14020347>.
  29. Wang Y, Li F, Zhang G, Kang L, Qin B, Guan H. Altered DNA methylation and expression profiles of 8-Oxoguanine DNA glycosylase 1 in Lens tissue from Age-related cataract patients. *Curr Eye Res*. 2015;40:815–21. <https://doi.org/10.3109/02713683.2014.957778>.
  30. Hunter A, Spechler PA, Cwanger A, Song Y, Zhang Z, Ying GS, Hunter AK, Dezoeten E, Dunaief JL. DNA methylation is associated with altered gene expression in AMD. *Invest Ophthalmol Vis Sci*. 2012;53:2089–105. <https://doi.org/10.1167/iovs.11-8449>.
  31. Oliver VF, Jaffe AE, Song J, Wang G, Zhang P, Branham KE, Swaroop A, Eberhart CG, Zack DJ, Qian J, et al. Differential DNA methylation identified in the blood and retina of AMD patients. *Epigenetics*. 2015;10:698–707. <https://doi.org/10.1080/15592294.2015.1060388>.
  32. Khuc E, Bainer R, Wolf M, Clay SM, Weisenberger DJ, Kemmer J, Weaver VM, Hwang DG, Chan MF. Comprehensive characterization of DNA methylation changes in Fuchs endothelial corneal dystrophy. *PLoS ONE*. 2017;12:e0175112. <https://doi.org/10.1371/journal.pone.0175112>.
  33. Young CH, Chiu YT, Shih TS, Lin WR, Chiang CC, Chou YE, Cheng YW, Tsai YY. E-cadherin promoter hypermethylation May contribute to protein inactivation in pterygia. *Mol Vis*. 2010;16:1047–53.
  34. Dianat T, Naiem Aminifard M, Arish M, Hussein Sangtrash M, Poyandeh R. Correlation between promoter hypermethylation and expression profiles of P15INK4b and P16INK4a genes on development of pterygium disease. *J Epigenetics*. 2021;2:25–30. <https://doi.org/10.22111/JEP.2020.31529.1015>.
  35. Park HS, Kim J, Ahn SH, Ryu HY. Epigenetic targeting of histone deacetylases in diagnostics and treatment of depression. *Int J Mol Sci*. 2021;22. <https://doi.org/10.3390/ijms22105398>.
  36. Kim H, Park SY, Lee SY, Kwon JH, Byun S, Kim MJ, Yu S, Yoo JY, Yoon HG. Therapeutic effects of selective p300 histone acetyl-transferase inhibitor on liver fibrosis. *BMB Rep*. 2023;56:114–9. <https://doi.org/10.5483/BMBRep.2022-0188>.
  37. Topper MJ, Vaz M, Marrone KA, Brahmer JR, Baylin SB. The emerging role of epigenetic therapeutics in immuno-oncology. *Nat Reviews Clin Oncol*. 2020;17:75–90. <https://doi.org/10.1038/s41571-019-0266-5>.
  38. Tan DT, Chee SP, Dear KB, Lim AS. Effect of pterygium morphology on pterygium recurrence in a controlled trial comparing conjunctival autografting with bare sclera excision. *Arch Ophthalmol*. 1997;115:1235–40. <https://doi.org/10.1001/archophth.1997.01100160405001>.
  39. Ryu HY, Zhao D, Li J, Su D, Hochstrasser M. Histone sumoylation promotes Set3 histone-deacetylase complex-mediated transcriptional regulation. *Nucleic Acids Res*. 2020;48:12151–68. <https://doi.org/10.1093/nar/gkaa1093>.
  40. Ryu HY, Su D, Wilson-Eisele NR, Zhao D, López-Giráldez F, Hochstrasser M. The Ulp2 SUMO protease promotes transcription elongation through regulation of histone sumoylation. *Embo J*. 2019;38:e102003. <https://doi.org/10.15252/emboj.2019102003>.
  41. Perna A, Alberi LA. TF-ChIP method for Tissue-Specific gene targets. *Front Cell Neurosci*. 2019;13:95. <https://doi.org/10.3389/fncel.2019.00095>.
  42. Liu Y, Park JM, Lim S, Duan R, Lee DY, Choi D, Choi DK, Rhie BH, Cho SY, Ryu HY, et al. Tho2-mediated escort of Nrd1 regulates the expression of aging-related genes. *Aging Cell*. 2024;e14203. <https://doi.org/10.1111/acer.14203>.
  43. Ryu HY, Lopez-Giraldez F, Knight J, Hwang SS, Renner C, Kreft SG, Hochstrasser M. Distinct adaptive mechanisms drive recovery from aneuploidy caused by loss of the Ulp2 SUMO protease. *Nat Commun*. 2018;9:5417. <https://doi.org/10.1038/s41467-018-07836-0>.
  44. Heintzman ND, Stuart RK, Hon G, Fu Y, Ching CW, Hawkins RD, Barrera LO, Van Calcar S, Qu C, Ching KA, et al. Distinct and predictive chromatin signatures of transcriptional promoters and enhancers in the human genome. *Nat Genet*. 2007;39:311–8. <https://doi.org/10.1038/ng1966>.
  45. Barski A, Cuddapah S, Cui K, Roh TY, Schones DE, Wang Z, Wei G, Chepelev I, Zhao K. High-resolution profiling of histone methylations in the human genome. *Cell*. 2007;129:823–37. <https://doi.org/10.1016/j.cell.2007.05.009>.
  46. Nickells RW, Zack DJ. Apoptosis in ocular disease: a molecular overview. *Ophthalmic Genet*. 1996;17:145–65. <https://doi.org/10.3109/13816819609057889>.
  47. Howe FS, Fischl H, Murray SC, Mellor J. Is H3K4me3 instructive for transcription activation? *BioEssays*. 2017;39:1–12. <https://doi.org/10.1002/bies.201600095>.
  48. Igolkina AA, Zinkevich A, Karandasheva KO, Popov AA, Selifanova MV, Nikolaeva D, Tkachev V, Penzar D, Nikitin DM, Buzdin A. H3K4me3, H3K9ac, H3K27ac, H3K27me3 and H3K9me3 histone tags suggest distinct regulatory evolution of open and condensed chromatin landmarks. *Cells*. 2019;8. <https://doi.org/10.3390/cells8091034>.
  49. Ninova M, Fejes Tóth K, Aravin AA. The control of gene expression and cell identity by H3K9 trimethylation. *Development*. 2019;146. <https://doi.org/10.1242/dev.181180>.
  50. Zhang T, Cooper S, Brockdorff N. The interplay of histone modifications - writers that read. *EMBO Rep*. 2015;16:1467–81. <https://doi.org/10.15252/embr.201540945>.
  51. Naik A, Dalpatraj N, Thakur N. Global gene expression regulation mediated by TGF $\beta$  through H3K9me3 mark. *Cancer Inf*. 2022;21:11769351221115135. <https://doi.org/10.1177/11769351221115135>.
  52. McCarthy RL, Kaeding KE, Keller SH, Zhong Y, Xu L, Hsieh A, Hou Y, Donahue G, Becker JS, Alberto O, et al. Diverse heterochromatin-associated proteins repress distinct classes of genes and repetitive elements. *Nat Cell Biol*. 2021;23:905–14. <https://doi.org/10.1038/s41556-021-00725-7>.
  53. Lu C, Yang D, Sabbatini ME, Colby AH, Grinstaff MW, Oberlies NH, Pearce C, Liu K. Contrasting roles of H3K4me3 and H3K9me3 in regulation of apoptosis and gemcitabine resistance in human pancreatic cancer cells. *BMC Cancer*. 2018;18:149. <https://doi.org/10.1186/s12885-018-4061-y>.
  54. Olcina MM, Leszczynska KB, Senra JM, Isa NF, Harada H, Hammond EM. H3K9me3 facilitates hypoxia-induced p53-dependent apoptosis through repression of APAK. *Oncogene*. 2016;35:793–9. <https://doi.org/10.1038/onc.2015.134>.
  55. Liu X, Zhang J, Nie D, Zeng K, Hu H, Tie J, Sun L, Peng L, Liu X, Wang J. Comparative transcriptomic analysis to identify the important coding and Non-coding RNAs involved in the pathogenesis of pterygium. *Front Genet*. 2021;12:646550. <https://doi.org/10.3389/fgene.2021.646550>.
  56. Moosavi A, Motevalizadeh Ardekani A. Role of epigenetics in biology and human diseases. *Iran Biomed J*. 2016;20:246–58. <https://doi.org/10.22045/ibj.2016.01>.
  57. Liu J, Jiang F, Jiang Y, Wang Y, Li Z, Shi X, Zhu Y, Wang H, Zhang Z. Roles of exosomes in ocular diseases. *Int J Nanomed*. 2020;15:10519–38. <https://doi.org/10.2147/ijn.S277190>.
  58. Jin YY, Liang YP, Huang WH, Guo L, Cheng LL, Ran TT, Yao JP, Zhu L, Chen JH. Ocular A-to-I RNA editing signatures associated with SARS-CoV-2 infection. *BMC Genomics*. 2024;25:431. <https://doi.org/10.1186/s12864-024-10324-z>.
  59. Jauregui-Lozano J, McGovern SE, Bakhle KM, Hagins AC, Weake VM. Establishing the contribution of active histone methylation marks to the aging transcriptional landscape of *Drosophila* photoreceptors. *Sci Rep*. 2023;13:5105. <https://doi.org/10.1038/s41598-023-32273-5>.
  60. Ma A, Zhao B, Boulton M, Albon J. A role for Notch signaling in corneal wound healing. *Wound Repair Regen*. 2011;19:98–106. <https://doi.org/10.1111/j.1524-475X.2010.00648.x>.
  61. Morin PJ, Sparks AB, Korinek V, Barker N, Clevers H, Vogelstein B, Kinzler KW. Activation of beta-catenin-Tcf signaling in colon cancer by mutations in beta-catenin or APC. *Science*. 1997;275:1787–90. <https://doi.org/10.1126/science.275.5307.1787>.
  62. Jones RG, Plas DR, Kubek S, Buzzai M, Mu J, Xu Y, Birnbaum MJ, Thompson CB. AMP-activated protein kinase induces a p53-dependent metabolic checkpoint. *Mol Cell*. 2005;18:283–93. <https://doi.org/10.1016/j.molcel.2005.03.027>.
  63. Chen Y, Wang H, Jiang Y, Zhang X, Wang Q. Transcriptional profiling to identify the key genes and pathways of pterygium. *PeerJ*. 2020;8:e9056. <https://doi.org/10.7717/peerj.9056>.
  64. Hou A, Lan W, Law KP, Khoo SC, Tin MQ, Lim YP, Tong L. Evaluation of global differential gene and protein expression in primary pterygium: S100A8 and S100A9 as possible drivers of a signaling network. *PLoS ONE*. 2014;9:e97402. <https://doi.org/10.1371/journal.pone.0097402>.
  65. Wolf J, Hajdu RI, Boneva S, Schlecht A, Lapp T, Wacker K, Agostini H, Reinhard T, Auw-Hadrich S, Schlunck G, et al. Characterization of the cellular microenvironment and novel specific biomarkers in pterygia using RNA sequencing. *Front Med (Lausanne)*. 2021;8:714458. <https://doi.org/10.3389/fmed.2021.714458>.
  66. Maddala R, Walters M, Brophy PJ, Bennett V, Rao PV. Ankyrin-B directs membrane tethering of periaxin and is required for maintenance of lens fiber cell hexagonal shape and mechanics. *Am J Physiol Cell Physiol*. 2016;310:C115–126. <https://doi.org/10.1152/ajpcell.00111.2015>.

67. Ulmer M, Li J, Yaspan BL, Ozel AB, Richards JE, Moroi SE, Hawthorne F, Budenz DL, Friedman DS, Gaasterland D, et al. Genome-wide analysis of central corneal thickness in primary open-angle glaucoma cases in the NEIGHBOR and GLAUGEN consortia. *Invest Ophthalmol Vis Sci*. 2012;53:4468–74. <https://doi.org/10.1167/iovs.12-9784>.
68. Kurji KH, Cui JZ, Lin T, Harriman D, Prasad SS, Kojic L, Matsubara JA. Microarray analysis identifies changes in inflammatory gene expression in response to amyloid-beta stimulation of cultured human retinal pigment epithelial cells. *Invest Ophthalmol Vis Sci*. 2010;51:1151–63. <https://doi.org/10.1167/iovs.09-3622>.
69. Shen-Gunther J, Wang CM, Poage GM, Lin CL, Perez L, Banks NA, Huang TH. Molecular pap smear: HPV genotype and DNA methylation of ADCY8, CDH8, and ZNF582 as an integrated biomarker for high-grade cervical cytology. *Clin Epigenetics*. 2016;8:96. <https://doi.org/10.1186/s13148-016-0263-9>.
70. Abusamak M, Issa SM, Alomari AF, Alsalamat HA, Haj Ali NS, Izmegna A, Shawashreh M, Abu Samak M, Abusamak TM. Corneal stromal mapping characteristics in normal Corneas using anterior segment SD-OCT. *Front Med (Lausanne)*. 2024;11:1485718. <https://doi.org/10.3389/fmed.2024.1485718>.
71. Mogal MR, Mahmud MR, Sompa SA, Junayed A, Abedin MZ, Sikder MA. Association between Ankyrin 2 gene and breast cancer progression: A preliminary computational assessment using the database approach. *Inf Med Unlocked*. 2021;25:100663.
72. Zhu L, Sun H, Tian G, Wang J, Zhou Q, Liu P, Tang X, Shi X, Yang L, Liu G. Development and validation of a risk prediction model and nomogram for colon adenocarcinoma based on methylation-driven genes. *Aging*. 2021;13:16600–19. <https://doi.org/10.18632/aging.203179>.
73. Zou B, Jiang W, Han H, Li J, Mao W, Tang Z, Yang Q, Qian G, Qian J, Zeng W, et al. Acyloxyacyl hydrolase promotes the resolution of lipopolysaccharide-induced acute lung injury. *PLoS Pathog*. 2017;13:e1006436. <https://doi.org/10.1371/journal.ppat.1006436>.
74. Barnes KC, Grant A, Gao P, Baltadjieva D, Berg T, Chi P, Zhang S, Zambelli-Weiner A, Ehrlich E, Zardkoohi O, et al. Polymorphisms in the novel gene acyloxyacyl hydroxylase (AOAH) are associated with asthma and associated phenotypes. *J Allergy Clin Immunol*. 2006;118:70–7. <https://doi.org/10.1016/j.jaci.2006.03.036>.
75. Zhang Y, Endam LM, Filali-Mouhim A, Zhao L, Desrosiers M, Han D, Zhang L. Polymorphisms in RYBP and AOA genes are associated with chronic rhinosinusitis in a Chinese population: a replication study. *PLoS ONE*. 2012;7:e39247. <https://doi.org/10.1371/journal.pone.0039247>.
76. Zhang W, Zhou M, Lu W, Gong J, Gao F, Li Y, Xu X, Lin Y, Zhang X, Ding L, et al. CNTNAP4 deficiency in dopaminergic neurons initiates parkinsonian phenotypes. *Theranostics*. 2020;10:3000–21. <https://doi.org/10.7150/thno.40798>.
77. Zhang W, Ding L, Chen H, Zhang M, Ma R, Zheng S, Gong J, Zhang Z, Xu H, Xu P, et al. Cntnap4 partial deficiency exacerbates  $\alpha$ -synuclein pathology through astrocyte-microglia C3-C3aR pathway. *Cell Death Dis*. 2023;14:285. <https://doi.org/10.1038/s41419-023-05807-y>.
78. Zhao X, Cao D, Ren Z, Liu Z, Lv S, Zhu J, Li L, Lang R, He Q. Dipeptidyl peptidase like 6 promoter methylation is a potential prognostic biomarker for pancreatic ductal adenocarcinoma. *Biosci Rep*. 2020;40. <https://doi.org/10.1042/bsr20200214>.
79. Nolan TM, DiGirolamo N, Sachdev NH, Hampartzoumian T, Coroneo MT, Wakefield D. The role of ultraviolet irradiation and heparin-binding epidermal growth factor-like growth factor in the pathogenesis of pterygium. *Am J Pathol*. 2003;162:567–74. [https://doi.org/10.1016/s0002-9440\(10\)63850-3](https://doi.org/10.1016/s0002-9440(10)63850-3).

#### Publisher's note

Springer Nature remains neutral with regard to jurisdictional claims in published maps and institutional affiliations.